# Iterative procedure for in-situ EUV optical testing with an incoherent source

Ryan Miyakawa* and Patrick Naulleau
*Lawrence Berkeley National Laboratory, Berkeley, CA 94720*

Avideh Zakhor
*Dept. of Electrical Engineering, UC Berkeley, Berkeley CA 94720*
(Dated: June 16, 2009)

We propose an iterative method for in-situ optical testing under partially coherent illumination that relies on the rapid computation of aerial images. In this method a known pattern is imaged with the test optic at several planes through focus. A model is created that iterates through possible aberration maps until the through-focus series of aerial images matches the experimental result. The computation time of calculating the through-focus series is significantly reduced by a-SOCS, an adapted form of the Sum Of Coherent Systems (SOCS) decomposition. In this method, the Hopkins formulation is described by an operator $S$ which maps the space of pupil aberrations to the space of aerial images. This operator is well approximated by a truncated sum of its spectral components.

PACS numbers:

## I. INTRODUCTION

As EUV optical systems move to larger numerical apertures to achieve higher resolution, it is crucial to have a simple and reliable procedure for characterizing the aberrations present in the optics. Standard interferometric techniques are more difficult to perform at higher numerical apertures. Reference wave interferometry such as PS/PDI requires smaller pinholes that are difficult to fabricate and provide low photon flux that gives poor contrast fringes [1]. Grating-based interferometry such as lateral shearing interferometry (LSI) is promising, but has strict tolerances on the position and tilt of the optical elements which couple with aberrations much more prominently at higher numerical apertures. Many iterative procedures have the benefit of being independent of numerical aperture, making them much more experimentally feasible. They also have the advantage that they can be made to work with existing tools with no additional experimental setup.

## II. SETUP AND PROCEDURE

A schematic representation of a typical EUV optical system is shown in Figure 1. Light radiates from an extended incoherent source placed in the rear focal plane of a collector optic that illuminates a test pattern, which is imaged by the test optic onto the detector. Here, the detector can either be a CCD camera in an imaging setup, or a resist-coated wafer in a lithography setup. We obtain a through-focus series of images by translating the detector stage in $z$ between each exposure. In a lithography tool, images are obtained by developing the photoresist and viewing them by a scanning electron microscope (SEM), using the commercial software SuMMiT to process and convert the images into binary line-edge profiles.

An important consideration is picking a test pattern that has a unique through-focus signature in response to the aberrations of interest of the test optic. For example, a test pattern containing only vertical lines may be a poor choice since it has a similar through-focus signature in response to aberrations that are symmetric about the $y$-axis, such as spherical aberration and secondary $x$-$y$ astigmatism (each of which has a 4th order $x$-dependence ). A proper test pattern will have a diffraction pattern that sufficiently probes the test optic pupil. If a case arises where certain aberrations are more important than others to detect, an appropriate test pattern can be designed to send the diffracted light at targeted angles.

A flow-diagram of the reconstruction algorithm is shown in Figure 2. A computer model of the optical system is generated using the known test pattern and source parameters. It has been shown [2] that the effect of resist blurring can be modeled as a linear system whose point-spread function is described by a host function with parameters that we allow to float in the algorithm. An aerial image through-focus series is generated via a-SOCS using a initial guess vector of aberrations. In the imaging setup, a merit function is generated by comparing the image series to the experimental aerial images. In the lithography setup, the image series is convolved with the resist point-spread function, thresholded and compared with the experimental line-edges. The aberration vector and host function parameters are modified using a hybrid simplex/simulated annealing algorithm whereby the best results from a set of independent trials is used as the initial guess of a subsequent generation of trials. The calculation is performed iteratively until the merit function reaches a desired tolerance.

*Electronic address: rhmiyakawa@lbl.gov

## III. FAST AERIAL IMAGE COMPUTATION

The robustness of the algorithm relies on the computation of many iterations, each of which involves the calculation of several aerial images. Aerial image modeling is normally computationally taxing because the Hopkins equation which governs the partially coherent imaging system requires integration across four variables. In order to make the reconstruction algorithm more computationally feasible, we develop a new method for aerial image calculation that leverages the specific configuration of our experiment to optimize the calculation.

### A. Motivation

In one dimension the Hopkins integral for aerial image calculation takes the following form:

$$\mathscr{I}(\nu) = \iint dp\, dz\, \mathscr{J}_0(p)\mathscr{K}(\nu)\mathscr{K}^*(\nu - z) \quad (1)$$
$$\times \mathscr{T}(\nu + p)\mathscr{T}^*(\nu - z + p) \quad (2)$$

Here $\mathscr{I}$ is the aerial image intensity Fourier transform, $\mathscr{K}$ is the coherent transmission function, $\mathscr{J}_0$ is the Fourier transform of mutual intensity of the light illuminating the mask and $\mathscr{T}$ is the mask Fourier transform. The Hopkins integral can be thought of as a system that takes three inputs, the mask, the source, and the pupil, and outputs the aerial image. In our experiment, the source and the mask are the same across all the calculations, so we can represent the Hopkins integral as a new system $S$ that has the source and mask information integrated in the system. We can now think of the system $S$ as mapping a pupil to an aerial image directly. Mathematically we can write this as

$$\mathscr{I}(\nu) = \int_{-\infty}^{\infty} dz\, \mathscr{K}(\nu)\mathscr{K}^*(\nu - z)S(\nu, \nu - z) \quad (3)$$

$$S(k, m) = \int_{-\infty}^{\infty} dp\, \mathscr{J}_0(p)\mathscr{T}(k + p)\mathscr{T}^*(m + p) \quad (4)$$

where $S$ is the system cross-coefficient (SCC) matrix, that depends only on the source and mask. This formulation is in direct analogy with the more familiar transmission cross-coefficients (TCC) which depend on the source and the pupil [3]. Since $S$ is a constant in each of the calculations, it can be computed once and stored, eliminating the need to evaluate it each time. We now show that by exploiting the mathematical structure of $S$, we can approximate it and significantly reduce the number of computations required to calculate the aerial image.

### B. Spectral decomposition of the SCC matrix

By direct analogy to the TCC matrix in [3], it can be shown that $S(k, m) = S^*(m, k)$ over the complex field so that $S$ is Hermitian. Spectral theorem therefore guarantees us that $S$ is diagonalizable and that we can write $S$ as a sum over the outer products of its eigenvectors weighted by their corresponding eigenvalues,

$$S(k, m) = \sum_{i=1}^{N} \lambda_i \xi_i(k)\xi_i^*(m) \quad (5)$$

where $N = rank\{S\}$, which can be shown to be equal to the number of sampled source points. Plugging back into (3), and swapping the order of the sum and integral gives:

$$\mathscr{I}(\nu) = \sum_{i=1}^{N} \lambda_i \int_{-\infty}^{\infty} dz\, [\mathscr{K}(\nu)\xi_i(\nu)][\mathscr{K}^*(\nu - z)\xi_i^*(\nu - z)]$$

We recognize the integral as the autocorrelation of the product $\mathscr{K}\xi_i$ and take the inverse Fourier transform of both sides to get the space-domain aerial image intensity.

$$I(x) = \sum_{i=1}^{N} \lambda_i |\mathscr{F}^{-1}\{\mathscr{K}\xi_i\}|^2 \quad (6)$$

### C. Truncation of the spectral sum

Due to the energy compaction property of spectral decomposition [4], the majority of the weight of $S$ is represented in a relatively small number of terms. The aerial image intensity is therefore well-approximated by considering only the first $K^* < N$ terms of the sum.

$$I(x) \approx \bar{I}(x) = \sum_{i=1}^{K^*} \lambda_i |\mathscr{F}^{-1}\{\mathscr{K}\xi\}|^2 \quad (7)$$

$K^*$ is chosen to give a specified tolerance on the aerial image computation. The normalized error $E$ between $I(x)$ and $\bar{I}(x)$ is bounded by the sum of the remaining eigenvalues:

$$E \leq \sum_{i=K^*+1}^{N} |\lambda_i| \quad (8)$$

We find that in a typical case, to achieve an error less than 1%, the value of $K^*/N \approx .1$ to $.15$, meaning that the aerial image computation is performed 7 to 10 times faster than with conventional methods.

## IV. SIMULATION AND DISCUSSION

We model a 0.35 NA imaging system operating at $\lambda = 13.5$ nm with a coherence factor $\sigma = 0.5$ in MATLAB. The test pattern is designed of a single pinhole of diameter $d = 50$ nm, which is chosen to sweep through the full extent of the test optic pupil under the given illumination. An aberration vector of the first 10 Zernike

polynomials is generated randomly using a Gaussian distribution with standard deviation $s_g = 0.25$ waves. Detector shot noise is modeled using Poisson photon statistics on a 16-bit camera. Aerial images at 3 focus steps are computed using a-SOCS and matched to the target image. A merit function is generated by integrating the absolute difference between the normalized image intensities. Each subsequent aberration vector guess is generated via a simulated annealing search, the details of which will not be discussed here but can be found in the literature [6]. The results in Figure 3 show the simulated test optic aberration map and the reconstructed aberration map to be in good agreement with total rms wavefront error $\mathcal{E}_{rms} = .04$ waves. The simulation was performed on a Pentium-D 2.4 GHz dual-core processor and completed in 134 s.

As with many iterative procedures, convergence of the algorithm can be susceptible to long computation times depending on the input parameters. Since non-convex searches like simulated annealing tend to converge much more slowly than convex algorithms, the computation of many generations may be required before a desirable tolerance is achieved. Additionally, since simulated annealing relies on random motion in the parameter space to step toward the solution, increasing the dimensionality of the space by including more Zernike polynomials can put further demands on the algorithm.

These drawbacks notwithstanding, it should be noted that feeding the algorithm a larger set of through-focus images or multiple illumination settings makes the contour of the merit function more convex, which helps the algorithm converge more quickly. Another key advantage of simulated annealing is that it can be partitioned into independent tasks that can be run in parallel on several processors.

In summary, our preliminary simulations verify the viability an iterative image-based approach to optical testing. Further work must be done in extending the simulation to a lithography setup to assess the feasibility of using the method to test lithography tools. As we continue to move toward higher resolution, iterative image-based optical testing is a promising alternative to interferometry and may play an important role in next-generation optical systems.

## Acknowledgments

The authors are grateful for support from the NSF EUV Engineering Research Center. Lawrence Berkeley National Laboratory is operated under the auspices of the Director, Office of Science, Office of Basic Energy Science, of the US Department of Energy.

[1] P. P. Naulleau, K. A. Goldberg, et al., Applied Optics 38 (35), 7252-63 (1999), "Extreme-ultraviolet phase-shifting point-diffraction interferometer: a wave-front metrology tool with subangstrom reference-wave accuracy"

[2] C. Ahn and H. Kim and K. Baik, SPIE proc., Vol. 3334, pg. 752-763, 1998, "A novel approximate model for resist process

[3] N. B. Cobb, Fast optical and process proximity correction algorithms for integrated circuit manufacturing, Ph.D. dissertation (Electrical Engineering and Computer Science, University of California, Berkeley, 1998).

[4] Kenji Yamazoe, J. Opt. Soc. Am. A Vol. 25, No. 12, December 2008, "Computation theory of partially coherent imaging by stacked pupil shift matrix"

[5] M. P. Rimmer, Applied Optics Vol. 13, No. 3, March 1974, "Method for Evaluating Lateral Shearing Interferograms"

[6] S. Kirpatrick, Journal of Statistical Physics, Volume 34, Numbers 5-6 / March, 1984, "Optimization by simulated annealing: Quantitative studies"

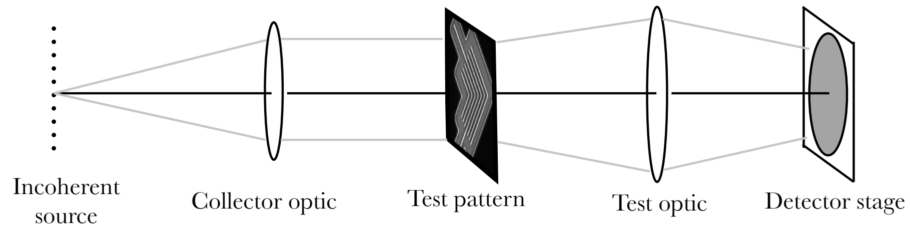


FIG. 1: A schematic representation of a typical EUV optical system

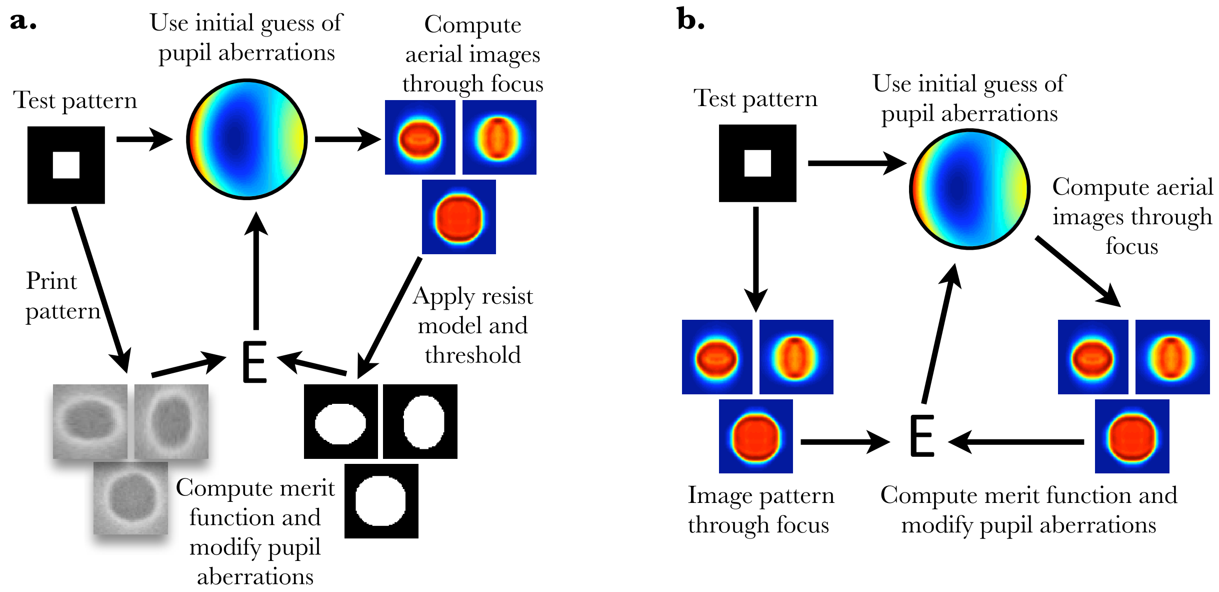


FIG. 2: (a) Flow diagram of iterative reconstruction algorithm for lithography setup. (b) Flow diagram for imaging setup

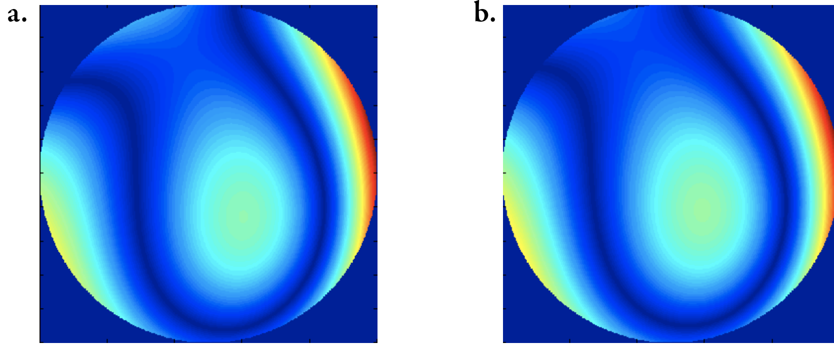


FIG. 3: a) Test wavefront. b) Reconstructed wavefront via iterative algorithm. Total rms wavefront error $\mathcal{E}_{rms} = .04$ waves